Porter-Thomas distribution in unstable many-body systems

Alexander Volya

Phys. Rev. C **83**, 044312 — Published 15 April 2011
DOI: 10.1103/PhysRevC.83.044312

Porter-Thomas distribution in unstable many-body systems

Alexander Volya
Department of Physics, Florida State University, Tallahassee, FL 32306-4350, USA
(Dated: March 25, 2011)

We use the continuum shell model approach to explore the resonance width distribution in unstable many-body systems. The single-particle nature of a decay, the few-body character of the interaction Hamiltonian, and the collectivity that emerges in non-stationary systems due to the coupling to the continuum of reaction states are discussed. Correlations between the structures of the parent and daughter nuclear systems in the common Fock space are found to result in deviations of decay width statistics from the Porter-Thomas distribution.

PACS numbers: 24.60.Lz, 24.10.Cn 24.60.Dr

I. INTRODUCTION

The Porter-Thomas distribution (PTD) [1] of transition strengths is a central aspect of complex systems. This statistical law was noted by many authors [2] to be valid more generally than other predictions of the Random Matrix Theory from which it originates. The PTD emerges under the assumption that the relative orientation of the two states involved in the overlap describing a transition covers the Ω-dimensional sphere in the Hilbert space uniformly. While this is true by definition of the Gaussian Orthogonal Ensemble (GOE), the validity of the PTD extends much farther as it constitutes the central limit theorem (CLT). Being a sum of a large number of uncorrelated components, the transitional amplitude is indeed expected to have a Gaussian (normal) distribution. There is a large volume of work on this subject; see reviews [2–6] and references therein. Generally, there is a consensus among authors that while the specifics of an ensemble and the physics of transitions do matter for certain observables, any deviations from the PTD are quickly defeated by even small stochastic components due to the robust nature of the CLT; see for example Ref. [7]. Any claims to the contrary, either experimental [8] or theoretical [9, 10], have always ignited debates and discussions [11].

Here we do not consider the data handling procedures which, on many occasions, have been deemed to be the most likely reasons for the deviations observed experimentally [6, 12]. Instead, we analyze the feasible scenarios with the help of the continuum shell model approach [13, 14], which is one of the best equipped methods to address the structure-reaction physics of interest microscopically. In a unified picture we review the superradiance (SR) effects [9, 15], the wave-function localization effects in the two-, three-, and four-body ensembles [16], the role of rotational symmetry, and other parent-daughter structural correlations that emerge in a decay [7].

The dynamics of an unstable many-body system projected onto the intrinsic space spanned by the bound (shell-model) states is generated by the effective, energy-dependent Hamiltonian [13, 17, 18]

$$\mathcal{H} = H - i \sum_{c(\text{open})} \wp^c \, |c\rangle\langle c|. \tag{1}$$

Here H is the Hermitian part that is identified with the traditional shell model Hamiltonian. The second, imaginary term reflects the irreversible decays into the continuum of states excluded by the Feshbach projection. This factorized operator contains the kinematic penetrability factor $\wp^c$ and the set of channel vectors $|c\rangle$. For simplicity we omit the angular momentum, isospin, and other labelings; detailed notations can be found in Ref. [13]. The problem is non-stationary; the Hamiltonian (1) is understood as a component of the propagator and is dependent on the scattering energy. The Hermitian component includes the coupling to the continuum of reaction states via virtual excitations; the penetrability also depends on energy through the kinematics of the decay process. Away from thresholds the energy dependence is smooth, and its exact form mainly pertains questions of the experimental data analysis [12]. We ignore this energy dependence here, and further assume that the penetrability $\wp$ is the same for all channels. The eigenvalues of the effective Hamiltonian (1) are complex, $\mathcal{E} = E - i\Gamma/2$, and represent the poles of the scattering matrix in the complex energy plane. These complex energies are associated with resonances and their widths.

Let us first consider weak decays, for which the imaginary component in Eq. (1) can be treated perturbatively. In this case the shell model eigenstate $|I\rangle$ defined by $H|I\rangle = E_I|I\rangle$ is not modified by the decay instability, and the corresponding decay width is

$$\Gamma_I = 2\wp\,\gamma_I, \quad \text{where} \quad \gamma_I = \sum_{c(\text{open})} |\langle I|c\rangle|^2$$

is the reduced width. The PTD of reduced widths,

$$P_\nu(\gamma) = \frac{1}{\gamma}\left(\frac{\nu\gamma}{2\overline{\gamma}}\right)^{\nu/2} \frac{1}{\Gamma(\nu/2)} \exp\left(-\frac{\nu\gamma}{2\overline{\gamma}}\right), \tag{2}$$

emerges under the uniform Hilbert space coverage assumption for $|I\rangle$. Here ν is the dimension spanned by the channel vectors, and $\overline{\gamma}$ is the average reduced width. For the orthogonal and normalized channels $\overline{\gamma} = \nu/\Omega$.

II. NUMERICAL STUDIES

A. Superradiance

In this work we examine situations with only one open channel. The strength of the continuum coupling is defined as the average decay width relative to the level spacing. Here we quantify this coupling by the parameter $\varkappa = \wp/\lambda$, where $\lambda^2 = \Omega^{-1}\mathrm{Tr}\left(H^2\right)$ is the variance of the density of states distribution of H.

In Fig. 1 we consider an example where H in (1) is that of the GOE. Here the PTD is reproduced numerically in the limit $\wp \to 0$. The imaginary component in (1) is factorized, which is pertinent to the unitarity of the scattering matrix. This non-Hermitian component, when large, gives rise to the collectivity often referred to as superradiance (SR). A similar collectivity due to the factorized Hermitian interaction describes giant resonances. The resulting deformed random ensembles are discussed in Refs. [2, 19, 20]. As coupling to the continuum increases, and $\varkappa$ becomes large, the resonances start to overlap, thus reorienting the intrinsic structure. This could be hypothesized to result in the PTD being violated [9]. We find, to the contrary, that the SR mechanism alone is unlikely to cause a significant change to the PTD. Indeed, for $\varkappa \ll 1$, the PTD simply follows from the definition of GOE. For $\varkappa \gg 1$, in analogy to the deformed ensembles, the Hilbert space is separated into the SR channel space, which is one-dimensional here with a single eigenstate $\mathcal{E} = -i\wp$, and the orthogonal statistical (compound resonance) space of dimension $\Omega - 1$. Because H is orthogonally invariant, the reduced-space dynamics is represented by the GOE. With the perturbation theory built in this limit one finds that the reduced widths for the compound resonances follow the PTD with $\overline{\gamma} = 1/(\Omega\varkappa^2)$. For large Ω the single SR state with a reduced width $\gamma_{SR} = 1 - \varkappa^{-2}$ has no effect on the PTD. Numerical studies shown in Fig. 1 confirms the PTD for both small and large values of $\varkappa$. The slight deviation for $\varkappa$ between 0.5 and 2 is due to a small fraction of very broad states with $\gamma > 10\overline{\gamma}$. This localized effect is shown in the inset of Fig. 1. This subset of exceptionally broad states is difficult to identify experimentally.

B. Two-body embedded random ensemble

In recent studies [8, 9] the deviations from the PTD have been inferred from the observation that the fit of distribution of the level widths with Eq. (2) results in an unphysical parameter $\nu < 1$. This, however could be a misleading criterion because the effective ν depends on the region being fitted. In figures that follow, for a better visual perspective, we show distributions of absolute values of amplitudes $x = \sqrt{\gamma/\overline{\gamma}}$ instead of $\gamma/\overline{\gamma}$. The PTD follows from the Gaussian distribution $P_G(x) = \sqrt{2/\pi}\exp\left(-x^2/2\right)$ of amplitudes. Curves, highly peaked (leptokurtic) compared to the Gaussian,

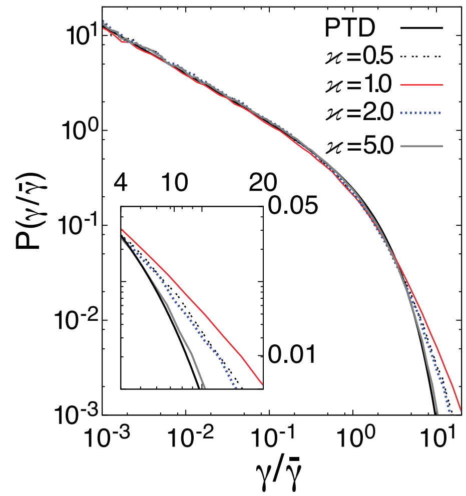

Figure 1: (Color online) The normalized distribution of probabilities of the reduced widths for ensemble with H in Eq. (1) being that of GOE; $\Omega = 10^4$. The curves for different continuum couplings $\varkappa = 0.5$, 1, 2, and 5 are compared with the PTD. The corresponding average widths $\Omega\overline{\gamma} = 0.76$, 0.40, 0.20, and 0.05, are computed after the very broad state(s) are removed from consideration. For $\varkappa > 2$ this amounts to exclusion of a single superradiant state in which case $\Omega\overline{\gamma} = \varkappa^{-2}$. With the exception of very broad states, there is perfect agreement with PTD, the differences being magnified in the inset where the region of $\gamma > 4\overline{\gamma}$ is shown. The largest deviation is observed for the transitional coupling strength $\varkappa = 1$. For $\varkappa = 5$ the distribution is already indistinguishable from the PTD.

correspond to an unphysical $\nu < 1$. One possible leptokurtic distribution, that we include in figures for the purposes of comparison, is provided by the Bessel function $P_B(x) = (2/\pi)K_0(x)$. In contrast to the Gaussian, the Bessel distribution emerges when the transitional overlap is possible only due to a single component in the wave-function along some direction in the Hilbert space given by a vector $|1\rangle$. Therefore $\langle I|c\rangle = \langle I|1\rangle\langle 1|c\rangle$, where both $\langle I|1\rangle$ and $\langle 1|c\rangle$ are distributed normally.

Experience with the realistic nuclear structure and some theoretical arguments [2–6] suggest that the effective Hamiltonian involves only few-nucleon interactions, thus, the two-body random ensembles (TBRE) appear to be more appropriate. While many features of these ensembles are different from those of GOE, numerical studies, in agreement with the CLT, confirm PTD of transition strengths toward an uncorrelated channel vector [7]. This, however, does not take into account the correlations that exist in the variable particle-number Fock space. Strong parent-daughter correlations emerge due to the microscopic physics of decay. Indeed, in the single-particle reaction processes all nucleons, except for one, are spectators, and the decay channels $|c;N\rangle$ for the $N-$particle system are built from the $(N-1)$-particle eigenstates of the daughter nucleus $|F;N-1\rangle$ that fol-

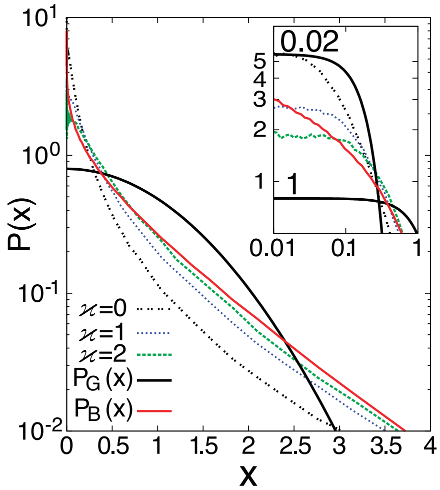

Figure 2: (Color online) The normalized distribution of probabilities of decay amplitudes in the TBRE ensemble with decay. The decay of a 7-particle system to the ground state of a 6-particle system is considered. There are 16 single-particle states, thus $\Omega = 11440$. The curves for different continuum couplings $\varkappa = 0$, 1, and 2 are compared with the Gaussian and Bessel distributions. The curves are normalized so that the average widths do not include the single SR state. $\Omega\overline{\gamma} = 1$, 0.19, and 0.06 for $\varkappa = 0$, 1 and 2 respectively. The region of very narrow widths is shown in the inset using a log-log scale. While all observed distributions for very narrow states seem to approach a constant, they are still not described by Gaussian distribution of different variances (or $\overline{\gamma}$'s). The inset includes two Gaussian curves with variances 1 and 0.02 as labeled.

low from the same two-body Hamiltonian. Thus,

$$|c; N\rangle = \left\{a^{\dagger}|F; N-1\rangle\right\}, \tag{3}$$

where $a^{\dagger}$ is a single-particle creation operator corresponding to the decaying nucleon, and brackets {...} indicate normalization to unity and appropriate symmetry coupling. The correlation between eigenstates and channels leads to the violation of PTD. Single-particle removal amplitudes are related to the independent-particle basis, where departure from the PTD has been demonstrated in the past [10].

In Fig. 2 we consider an ensemble where H in Eq. (1) is given by TBRE and does not include any symmetries. From Fig. 2 we find that none of the results follow the PTD. In contrast to the Gaussian curve $P_G(x)$ the distributions have sharp peaks at low amplitudes and an extended exponential tail. In the SR limit of large $\varkappa$ the distributions appear to approach the one given by the Bessel function $P_B(x)$.

C. k-BRE in single j model

The rank of the force beyond the two-body interaction, and symmetries, such as rotational, may have additional influences. To examine this we consider a model where N identical fermions occupy a single-j level. This has been a popular model for exploring the properties of TBRE with symmetries [3, 4, 21]. The resemblance of the low-lying spectra to those observed in realistic nuclei is the most intriguing feature. For our demonstration we select $j = 19/2$ and discuss widths of the decay of many-body states in 9-particle systems. The final state is the ground state of the system with 8 nucleons. All states, in both parent and daughter nuclei, are eigenstates of the same Hamiltonian given by the $k-$body Random Ensemble (k-BRE) [22]. In this work we restrict our consideration to the two-, three-, and four-body forces, i.e. $k = 2, 3$, and 4, respectively. We select only those realizations where the daughter system has ground state spin $F = 0$; and thus the channel spin is $I = 19/2$. The fractions of such realizations are 42%, 64%, and 83% for $k = 2, 3$, and 4 respectively.

The resemblance between random ensembles with symmetries and realistic nuclei extends to parentage relations. The low-lying states in the odd-particle parent nucleus are predominantly of the single-particle nature. If $F = 0$ for the even-particle core then the ground state of a system with an extra nucleon is likely to carry the single-particle quantum numbers $j = I = 19/2$. This is indeed observed, and the corresponding probabilities are 21%, 47%, and 37% for $k = 2, 3$, and 4 respectively. The correlation between the parent and daughter ground states is demonstrated in Fig. 3 which shows the distribution of reduced widths for the decay from ground state to ground state when $F = 0$ and $I = 19/2$. Both parent and daughter systems have correlated structures because they are eigenstates of the same Hamiltonian for different number of particles. In the distribution of spectroscopic factors this correlation is seen as a peak near $\gamma = 1$. As the rank of interaction k becomes higher, more remote configurations can be admixed, which reduces the ground state to ground state transitional collectivity. For totally uncorrelated systems the transitional strength due to the CLT is expected to follow the PTD.

Since most of the transitional strength is concentrated in a few states at the low end of the spectrum, here the PTD is not expected; however, there is also no agreement with this law for the widths of narrow compound resonances higher in the excitation spectrum. In Fig. 4 the distribution of reduced decay amplitudes is shown for the two-, three-, and four-body random ensembles with rotational symmetry. The curves are quite close to each other and are similar to the $\varkappa = 0$ result in Fig. 2. All findings indicate violation of the PTD.

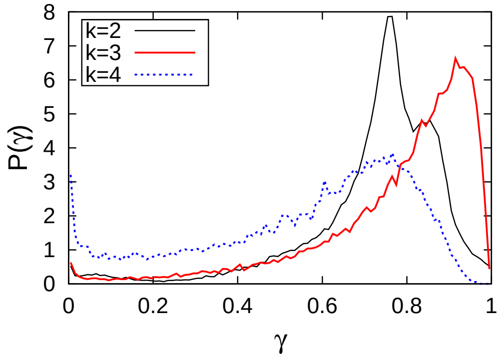

Figure 3: (Color online) Distribution of the reduced decay widths (spectroscopic factors) for the ground state $N = 9$ spin $I = 19/2$ parent decaying to the ground state $N = 8$ spin $F = 0$ daughter system. The k-BRE of identical nucleons in $j = 19/2$ level is considered. Three curves correspond to two-, three-, and four-body ($k = 2, 3,$ and 4) random ensembles with rotational symmetry.

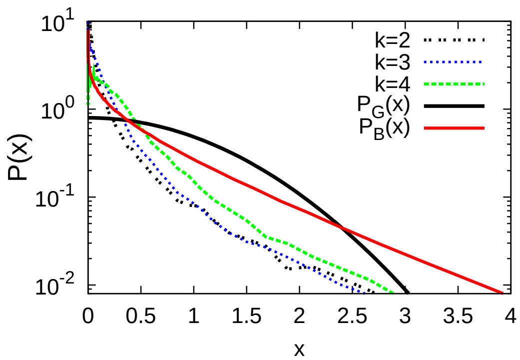

Figure 4: (Color online) Same model as in Fig. 3. The distribution of spectroscopic amplitudes for all 204 states with spin $I = 19/2$ in the parent 9-nucleon system is shown for the decay to the spin $F = 0$ ground state of the daughter nucleus. The results are compared with the Gaussian and Bessel distributions.

D. Distribution of electric $B(E2)$ rates

We attribute the deviations from the PTD seen in our numerical experiments to the parent-daughter relation in the particle decay process, namely that the structure of the parent eigenstate is correlated with that of the channel via Eq. (3). A similar, but perhaps less pronounced, behavior is expected for the electromagnetic decays, where channel

$$|c; N\rangle = \{\mathcal{M}|F; N\rangle\}$$

is constructed from a one-body multipole density operator $\mathcal{M}$. This is confirmed by the results shown in Fig. 5 which shows the distribution of amplitudes for electric quadrupole transitions. For this simple model space the effective charge and the radial overlap only define

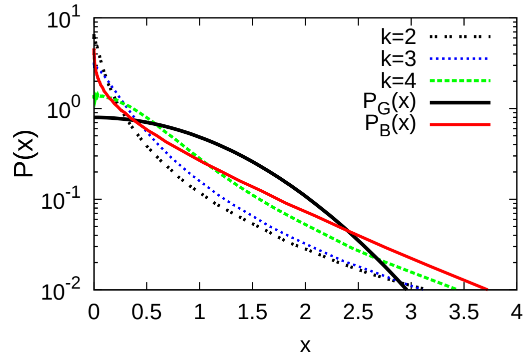

Figure 5: (Color online) Same $j = 19/2$ model as in Figs. 3 and 4. The distribution of reduced amplitudes $x = \sqrt{\gamma/\overline{\gamma}}$ with $\gamma = B(E2, 2 \to 0)$ being the reduced electric quadrupole transition rate from the $I = 2$ states to the $F = 0$ final ground state. The system with 8 nucleons is considered. The dotted curves correspond to two-, three-, and four-body ($k = 2, 3,$ and 4) random ensembles with rotational symmetry. The results are compared with the Gaussian and Bessel distributions.

an overall normalization, which is irrelevant for our purposes. Thus the reduced width can be assumed to coincide with the reduced electric quadrupole transition rate $\gamma = B(E2, 2 \to 0)$. Due to the presence of realizations with collective quadrupole transitions there are a few broad states that lead to noticeable deviations from the PTD in the $x > 1$ region. However, similar to the particle decay in Fig. 4, the deviations are seen throughout the entire range of widths.

III. ANALYSIS AND SUMMARY

The coefficient of variation $t^2 = \left(\overline{\gamma^2} - \overline{\gamma}^2\right)/\overline{\gamma}^2$ is commonly used as a measure of peakedness in a distribution of non-negative quantities. For PTD $t^2 = 2/\nu$; and $t^2 = 2$ for the Gaussian distribution of amplitudes can be compared with $t^2 = 8$ for the Bessel distribution. The coefficient of variation is equivalent to the excess kurtosis for the amplitudes x which is $t^2 - 2$. The excess kurtosis is positive for leptokurtic curves. In cases with collectivity, $\overline{\gamma}$ is disproportionately large due to the statistically unimportant collective state(s) far in the tail of the distribution, which has an adverse effect on t being used as a measure of peakedness [23]. To quantify the results we use a coefficient of L-variation, also known as the Gini coefficient,

$$\tau = \frac{1}{2\overline{\gamma}} \iint_0^\infty d\gamma d\gamma' |\gamma - \gamma'| P(\gamma) P(\gamma').$$

Although similar to the coefficient of variation, τ is less sensitive to the extremes in a distribution's tail [24]. τ ranges from 0 to 1. For the PTD with $\nu = 1, 2,$ and 3 the coefficient is $\tau = 2/\pi,\ 1/2,$ and $3/(4\pi)$, respectively. Thus

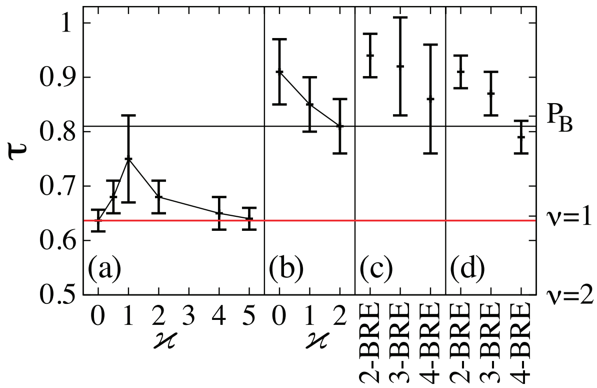

Figure 6: (Color online) The coefficient of L-variation for the models discussed in this work. (a) τ as a function of continuum coupling $\varkappa$ for the model in Sec. II A; (b) τ in TBRE discussed in Sec. II B as a function of $\varkappa$; (c) single j level model with particle decay, Sec. II C, coefficient of L-variation for the two-, three-, and four-body random ensembles; (d) same model as in (c) but τ is for the electric quadrupole transitions discussed in Sec. II D. The uncertainty shown reflects the finite sample size and sensitivity to the 1% of the data in the tail of the distribution. Horizontal grid-lines show the values of τ for PTD with $\nu = 2$ and 1, and for the Bessel distribution $P_B(x)$.

$\tau > 0.64$ is considered unphysically peaked. The Bessel distribution $P_B(x)$ with $\tau = 0.81$ is peaked. In Fig. 6 we summarize our model studies using the coefficient of L-variation. The uncertainty quoted is due to the finite sample size and to sensitivity to 1% of the data in the tail of the distribution. The results of the L-variation analysis in Fig. 6 confirm deviations from PTD observed in the models examined.

To summarize, this study is motivated by the long-standing debate in relation to the Porter-Thomas distribution and possibility of its violation [7–11]. The PTD is a robust prediction justified by the central limit theorem; it is easily confirmed for different random matrix ensembles. This, however, is a purely structural approach that does not take into account the microscopic physics of reactions. To address this we use a continuum shell model approach where violations of the PTD may result from one or a combination of the following: coherence in structure due to the factorized nature of the effective Hamiltonian that reflects unitarity of the scattering matrix, the so called superradiance mechanism; parent-daughter relation between decaying systems in the common Fock space; few-body low rank interaction forces; and significant variations in the energy dependence of the effective Hamiltonian. We examine all of these possibilities, with the exception of the last, which is to be discussed elsewhere.

The distribution, unambiguously different from the PTD, is observed in random ensembles with a particle and electromagnetic decays and with few-body intrinsic Hamiltonians. There are significant local deviations from the PTD in the wide region of spectrum where the strength function for the corresponding channel is significant. The parent-daughter relation in the decay process appears to be central to this phenomenon. From the perspective of the compound nucleus reaction mechanism, which is associated with the PTD, this picture is different because the two-body or other low-rank Hamiltonian does not lead to dynamical mixing of states strong enough for the decaying system to lose all memory of its creation. The formal analysis using the coefficient of L-variation is summarized in Fig. 6.

The author is thankful to Kirby Kemper for motivating discussions. Support from the U. S. Department of Energy, grant DE-FG02-92ER40750 is acknowledged. The computing resources were provided by the Florida State University shared High-Performance Computing facility.

[1] C. E. Porter and R. G. Thomas, Phys. Rev. **104**, 483 (1956).
[2] T. A. Brody, J. Flores, J. B. French, P. A. Mello, A. Pandey, and S. S. M. Wong, Rev. Mod. Phys. **53**, 385 (1981).
[3] V. Zelevinsky and A. Volya, Phys. Rep. **391**, 311 (2004).
[4] T. Papenbrock and H. A. Weidenmüller, Rev. Mod. Phys. **79**, 997 (2007).
[5] G. E. Mitchell, A. Richter, and H. A. Weidenmüller, Rev. Mod. Phys. **82** (2010).
[6] H. A. Weidenmüller and G. E. Mitchell, Rev. Mod. Phys. **81**, 539 (2009).
[7] S. M. Grimes, Phys. Rev. C **28**, 471 (1983).
[8] P. E. Koehler, F. Bečvář, M. Krtička, J. A. Harvey, and K. H. Guber, Phys. Rev. Lett. **105**, 072502 (2010).
[9] G. L. Celardo, N. Auerbach, F. M. Izrailev, and V. G. Zelevinsky, Phys. Rev. Lett. **106**, 042501 (2011).
[10] R. R. Whitehead, A. Watt, D. Kelvin, and A. Conkie, Phys. Lett. B **76**, 149 (1978).
[11] E. S. Reich, Nature **466**, 1034 (2010).
[12] H. A. Weidenmüller, Phys. Rev. Lett. **105**, 232501 (2010).
[13] A. Volya, Phys. Rev. C **79**, 044308 (2009).
[14] A. Volya and V. Zelevinsky, Phys. Rev. C **67**, 054322 (2003).
[15] A. Muller and H. L. Harney, Phys. Rev. C **37**, 2435 (1988).
[16] L. Kaplan and T. Papenbrock, Phys. Rev. Lett. **84**, 4553 (2000).
[17] H. Feshbach, *Theoretical nuclear physics : nuclear reactions* (Wiley, New York, 1991).
[18] C. Mahaux and H. A. Weidenmüller, *Shell-model approach to nuclear reactions* (North-Holland Pub. Co., Amsterdam, London, 1969).
[19] A. Pandey and J. B. French, J. Phys. A **12**, L83 (1979).
[20] V. V. Sokolov and V. G. Zelevinsky, Phys. Lett. B **202**, 10 (1988).
[21] C. W. Johnson, G. F. Bertsch, and D. J. Dean, Phys. Rev. Lett. **80**, 2749 (1998).
[22] A. Volya, Phys. Rev. Lett. **100**, 162501 (2008).
[23] F. J. Dyson, J. Royal Stat. Soc. **106**, 360 (1943).
[24] J. R. M. Hosking, J. Royal Stat. Soc., Ser. B **52**, 105 (1990).